論　文

A Study on the Most Suitable Shape of 3-Dimensional Bottom Roughness with Directional Resistance Properties

S. G. Gug[*]

방향성 저항특성을 가진 3차원 저면조도의 최적형상에 관한 연구

국　승　기

Abstract

In order to improve the water quality in semi-enclosed bays, Gug et al. (1997) have proposed a new method to activate the tidal exchange by creation and control of tidal residual current through the addition of artificial elements to create bottom roughness with directional resistance properties.

A design of tidal residual current is realized by arranging many units of desired shape to create artificial bottom roughness, so, it is advisable to arrange as few of these as possible from a point of cost-benefit view.

This paper attempts to develop the most suitable shape of artificial bottom roughness units with which to create and control an optimal tidal residual current. Several simple shapes were examined as fundamental cases. Subsequently 38 types of artificial bottom roughness units based on a few simple effective shapes, were examined experimentally.

As a result of this research, two types to create artificial roughness.

---

* 정회원, 한국해양대학교 해양경찰학과 교수

1. Introduction

Recently, water pollution in stagnant sea areas, such as semi-enclosed bays, has been recognized as one of the more serious water environmental

Fig. 1   Creation and control of tidal residual current by bottom roughness

problems. In order to activate the tidal exchange, *Komatsu et al.* (1997) proposed a new method to create and control the tidal residual current by creating artificial 3-dimensional unsymmetrical bottom roughness with directional resistance properties (see *FIG. 1*). Since this method is operated by natural tidal energy, it is possible to purify water quality over a large sea area with no maintenance cost. It has been supposed that the bottom roughness should be relatively small and that its height be limited to 10-15% of the water depth for safe navigation.

It was found that the tidal residual current could be controlled by arrangements of many
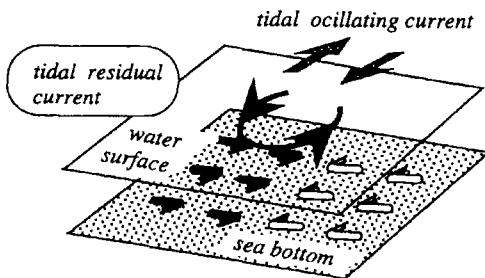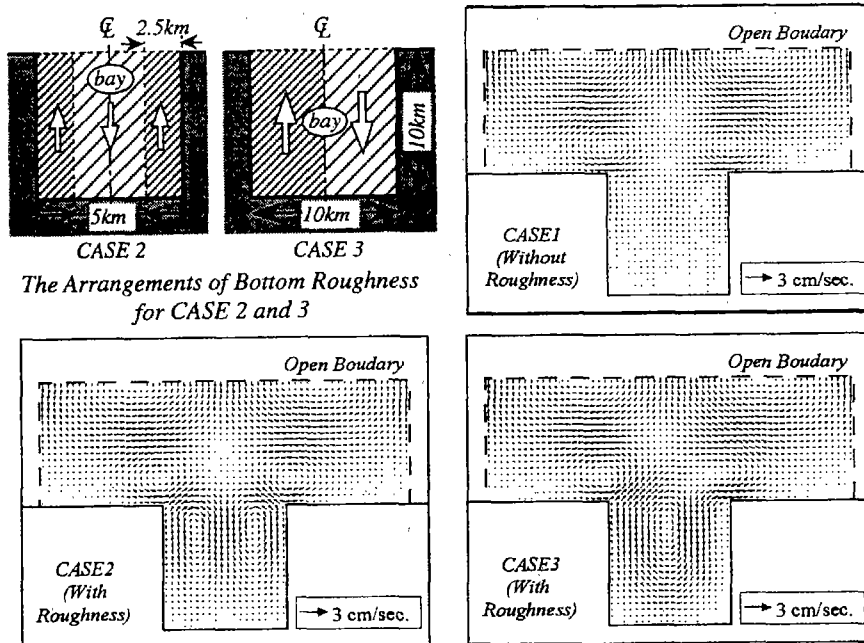

Fig. 2   Calculated results of tidal residual current
   The bottom roughness are set in the shaded area of the top left figures. Arrows mean the flow direction with smaller resistance and it is expected that the tidal residual current occurs along them. (The difference of resistance was taken by the difference of bottom friction coefficient evaluated experimentally by Gug et al.(1997) into account.)

units of artificial bottom roughness in a bay so as to produce arbitrary flow patterns and even combine or separate some original current circulations.

The calculated results of tidal current simulations with/without bottom roughness are shown in FIG. 2. It is seen from the comparison between CASE 1(no roughness case) and CASE 3(with roughness) that the clockwise tidal residual circulation is created by the bottom roughness in the bay. Furthermore, the comparison between CASE 2 and CASE 3, which have quite different arrangements of bottom roughness, suggests the possibility of designing arbitrary flow patterns by this method.

Many bottom roughness units are necessary to control the tidal residual current, as mentioned above. Therefore, it is necessary to find an available shape of unit with a greater ability to create the desired tidal residual current. In this paper, the most suitable shape of bottom roughness unit was examined. The difference of the resistance of bottom roughness due to flow directions, which is caused by an unsymmetrical body of bottom roughness, can generate the tidal residual current in the tidal current direction. Hence, the most suitable shape of bottom roughness unit is expected to have the largest difference of directional resistance.

2. Experimental Frame

2.1 Experimental Setup

The drag of bottom roughness was directly measured by the drag measuring device to find the model with larger difference between "backward" and "forward" forces. Here the "backward" means the flow direction with the larger resistance and the "forward" is the opposite direction, respectively. The schematic diagram of the experimental flume is shown in FIG. 3. It is 6.0m long, 0.5m wide, 0.5m tall and keeps the drag measuring device (see FIG. 4) on the center of the channel bed. The drag measuring device consists of an aluminium plate on which each roughness model can be set and has three supports. The drag force of the roughness is measured by two strain gauges fixed on the both sides of the downstream support as shown in FIG. 4. The water level is controlled by the movable weir at the downstream edge of the flume.
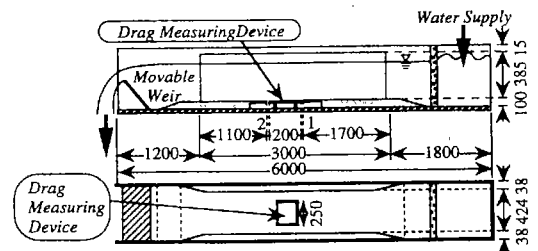

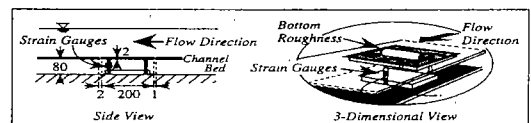Fig. 3   Schematic diagram of the experimental setup (unit : mm)

Fig. 4   Schematic diagram of the drag measuring device (unit : mm)

2.2 Measurement of Drag Coefficient Cd

The drags of each bottom roughness type were measured in both the backward and the forward directional flows. At first, the forward and the

Table 1 Summary of experiments for the fundamental shapes of the roughness

run	Roughness Type	Parameter	Frame of Roughness Model (Unit : cm)
run $\theta 1$	the Lying Cylinder Type	Opening Angle θ =120, 150, 180, 210, 240 degrees	Radius r=7.5, Width b=20, Thickness t=0.3
run $\theta 2$	the Standing Cylinder Type	θ =90, 120, 150, 180, 210, 240 degrees	r=10, b=5, t=0.3
run $\theta 3$	the Quarter Sphere Type	θ =60, 90, 120, 150 degrees	r=7.5, t=0.3
run $k\theta$	the Half Sphere Type	Relative Height k/D= 0.5, 0.7, 0.9, 1.0	Diameter d=15, t=1

backward drags D_f, D_b and the shear force on the plate without roughness F were measured. The drags in terms of only bottom roughness τ_f, τ_b were evaluated from the subtraction of F from D. Here, the subscripts f and b indicate the forward and the backward direction, respectively. The water depth h is defined as an average of 2 measurements at the upstream and the downstream of roughness points by the water level indicator. The drag coefficient of roughness is defined as

$$Cd \equiv \frac{\tau}{\frac{1}{2}\rho A U^2} \qquad (1)$$

where τ : the drag of a roughness, ρ : the density of water, A : the projected area of roughness on the perpendicular plane to the flow direction and U : the cross-sectional average velocity (=Q/hB, B=42.4cm)

3. Experimental Results

3.1 Fundamental Shapes of Bottom Roughness Units

If we place a half cylinder or a quarter cylinder, which is known as the best shape of 2-dimensional roughness(Awaya et al., 1995), on the bottom, we may get the noticeable change of drag. However, it is preferable to develop a more suitable 3-dimensional shape than a 2-dimensional shape because the resistance properties of the former are quite different. Thus, we tried to examine the characteristics of a few fundamental 3-D shapes of bottom roughness units as the first step of this research.

Two types of cylinder, namely, (1) the Lying Cylinder (: a cylinder laid on the bed) and (2) the Standing Cylinder (: a cylinder stood on the bed) were chosen as basic models, and the resistance properties of each were systematically investigated, using the Robinson cup anemometer which effectively creates a directional rotation by hemispherical shaped wind cups. In addition, sphere shapes were also examined by analogy with the Robinson cup. The summary of experiments is described in *Table 1* and *FIG. 5*. The experimental conditions are as follows : the relative water depth h/k=5, the water discharge Q=0.034 (m³/s) and Reynolds number Re=Uh/ν ≒ 80000. These Experimental results are presented in *FIG. 6*. As a result of run θ1, it becomes clear
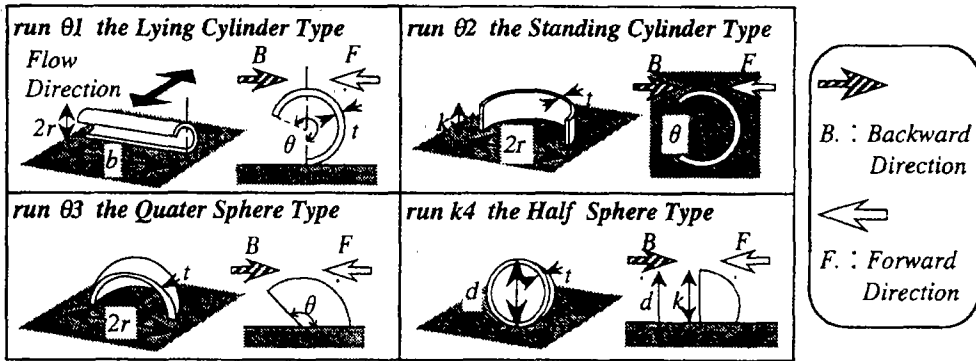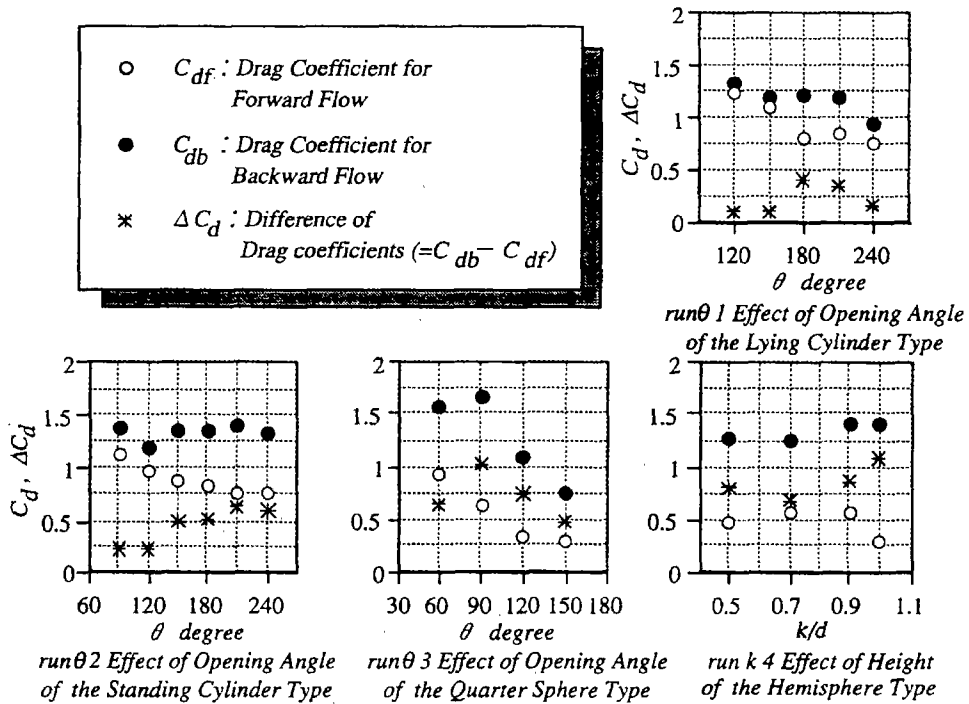
Fig. 5 Schematic diagram of fundamental roughness

Fig. 6 Experimental results in cases of fundamental shapes

that there is no distinct difference of drag coefficients ΔC_d when θ is smaller than 150degrees and that ΔC_d has a maximum value at $\theta = 180$ degrees.

As for the Standing Cylinder Type (run $\theta 2$), Δ C_d has the largest value when θ is 210 degrees. It is seen from those results that the resistance property of the lying cylinder type depends on the opening angle. Furthermore, the result of run $\theta 3$ indicates that ΔC_d has a maximum peak at $\theta = 90$

degrees as well as the value of C_{db}. It becomes clear from *run k4* that Cdf decreased with the increase of *k/d* and that the Hemisphere Type (k/d=1) has the largest value of ΔC_d.

It follows from these experiments that the better shapes with greater ΔC_d is the half cylinder for the Lying Cylinder Type and that the cylinder with the opening angle of 210 degrees for the Standing Cylinder Type, and that the hemisphere for the Sphere Type.

3.2 Improvement of Fundamental bottom Roughness Model

The 38 shapes were proposed on the basis of the above findings and were used to examine the resistance properties. Only the representative 9 models, which are categorized into 3 groups, are shown in *FIG. 7,* in which a 3-dimensional view, a side view, a front view from the upstream side of the backward flow and a plane view are placed clockwise for each model.

Type 1 is a half cylinder expected to be the most effective shape among lying cylinder types, while *Type 2* and *3* are the modified types of half cylinders. *Type 2* looks like "V" which is formed by combining 2 half cylinders. As for *Type 3,* a straight wing is added on a half cylinder to weaken the resistance in the forward direction.

Next, *Type 4, 5* and *6* belong to the sphere
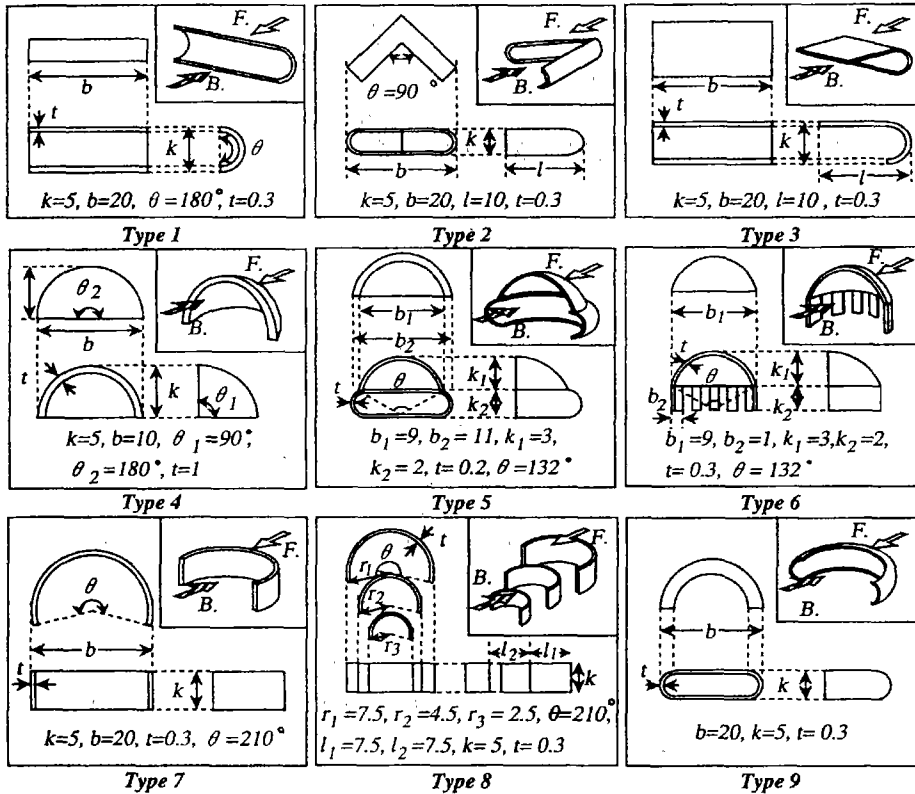

Fig. 7　The proposed roughness models (unit：cm)

group. **Type 4** is a quarter sphere model. **Type 5** is a quarter sphere attached to a half tire. As for **Type 6**, a part of quarter sphere on a standing half cylinder with some slits. **Type 7, 8** and **9** are included in a group of standing cylinder model. **Type 7** is a single cylinder. **Type 8** consists of three cylinders whose sizes are different so that the outline forms a streamlined body. **Type 9** is a shape like a half tire.
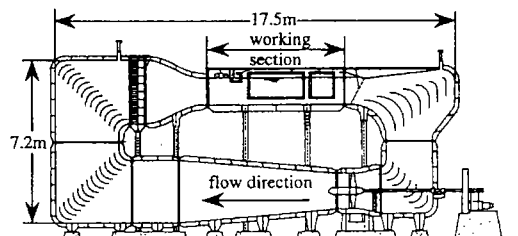
3.3 The Influences of Relative Depth and Reynolds Number on Cd

Before we measured drag coefficients of roughness fixed on the channel bed to choose the best shape, some preliminary experiments (see *TABLE 2*) had been carried out to clarify the relationships among C_d, and 2 important parameters, that is, the relative depth and the Reynolds number.

Table 2 Experimental conditions

run	Reynolds Number	Relative Depth (h/k)	Roughness Type No.
run R	3×10^4 to 1×10^6	6	1, 4, 7
run h	8×10^4	3 to 8	2, 3, 4

Two experimental flumes were used for *run R* to examine the effect of Reynolds number. One is a straight open channel which was introduced in the above mentioned experiments (see *FIG. 3*) and was used for the lower range of Reynolds number (3×10^4 to 1×10^5). The other is a circulating tank (see *FIG. 8*) for higher Reynolds number.

The results of **Type 4** are shown in *FIG. 9* as a typical example. It is seen that C_{df} and C_{db} tend to decrease with the increase of Reynolds number, and they gradually approach the constant values

Fig. 8 Experimental flume for run R : working section : 6.0m along, 2.0m wide, 1.2m deep

in the region $Re > 10^5$. This tendency was common to all roughness.

Secondly, the water depth was changed to explore the dependence of C_d on the relative depth (*run h*). The measured results of **Type 2** are shown in *FIG. 10*. The values of C_d monotonously fall off with the increase of h/k. The main reason is that the ratio of the area occupied by the roughness to the cross-section decreases with the increase of h/k. The value of ΔC_d considerably depends on h/k in the same way. Therefore, it is found that h/k is a very important parameter.

3.4 Comparison among Roughness Models

Judging from the above, the Reynolds number and the relative depth are required to be changed in order to compare roughness models in detail.

The experimental conditions are shown in *TABLE 3*. *FIG. 11* summarizes the results of ΔC_d in run 1, 2 and 3. C_{df} and C_{db} with the conditions that h/k is 5 and that Re is about 70000 are shown in *FIG. 12*. It becomes clear that **Type 5** and **Type 6** generate larger ΔC_d than other types and that especially the values of C_{db} of both types are large. As a result, **Type 5** and **Type 6** are expected to be effective shapes.
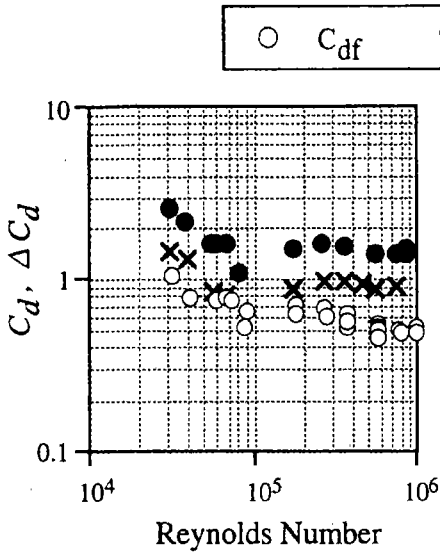
On the other hand, it is expected that the most

Fig. 9 Experimental results of
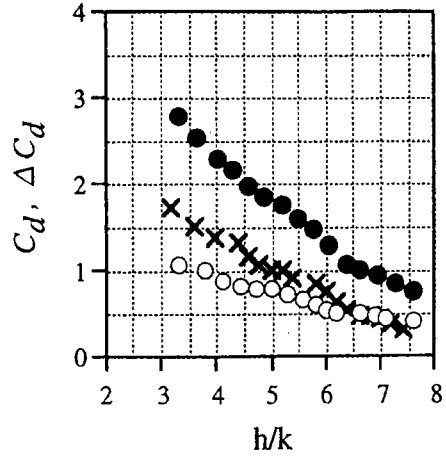run R for type 4

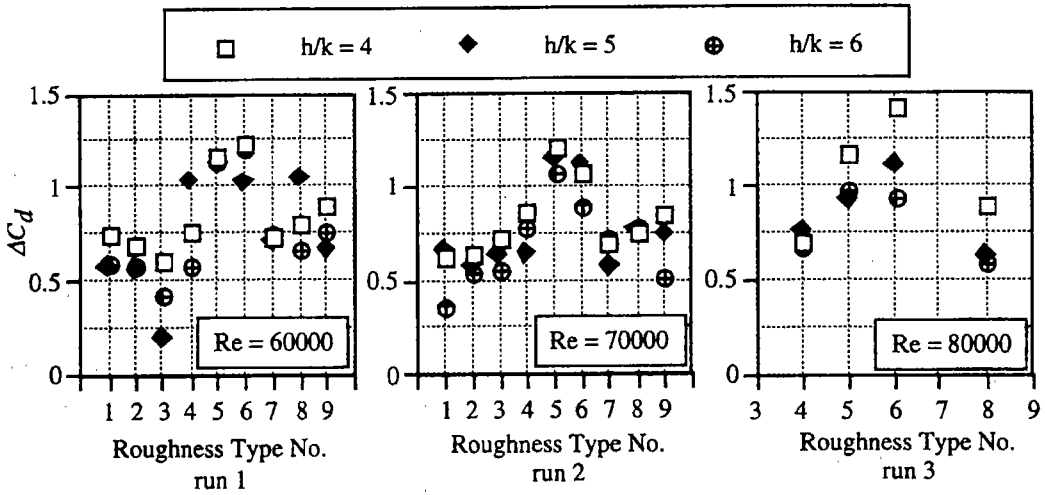Fig. 10 Experimental results of
run h for type 2

Fig. 11 ΔCd of each roughness model type

Table 3 Experimental Conditions

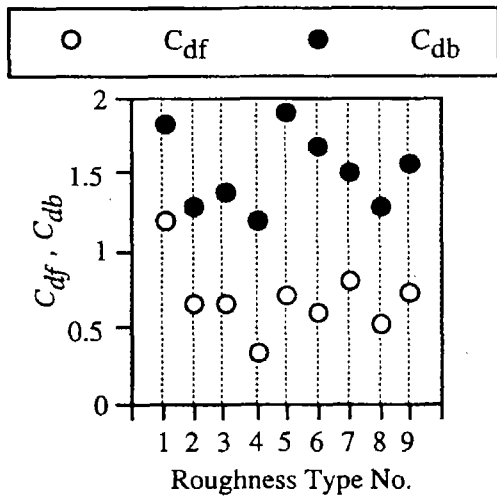| run	Reynolds Number	Relative Depth (h/k)	Roughness Type No.
1	6×10^4	4, 5, 6	1 to 9
2	7×10^4	4, 5, 6	1 to 9
3	8×10^4	4, 5, 6	4, 5, 6, 8

Fig. 12 C_{df} and C_{db} of each roughness model type (Re=700100, h/k=4)

efficient model can create an available tidal residual current with minimum loss of tidal energy. If some roughness models have the same value of ΔC_d, the shape with the smallest C_{df} is considered to be the most available model. Thus, the ratio of the difference of the drag coefficients to the forward drag coefficient

$$\alpha \equiv \frac{\Delta C_d}{C_{df}} = \frac{C_{db} - C_{df}}{C_{df}} \qquad (2)$$

is introduced as a new index for the rating. The experimental results of run 1, 2 and 3 are compared again using the rating index α in FIG. 13. The values of α are distributed over the rather wide range and **Type 4, 5, 6** and **8** get

relatively large values of α. For the reasons mentioned above, **Type 5** and **Type 6** can be proposed as the most suitable shapes.
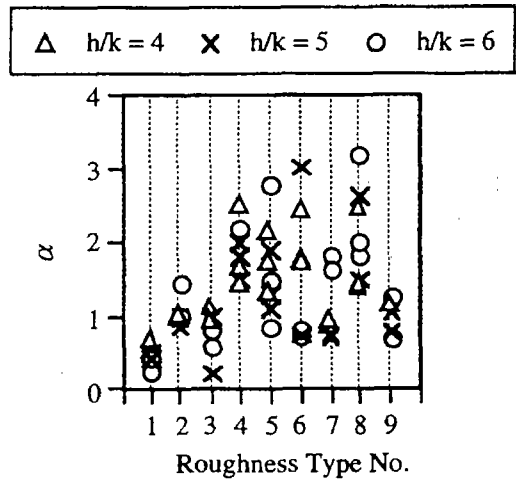

Fig. 13 α of each roughness model type

4. Conclusion

The results of these experiments can be as follows:

1) For the Lying Cylinder Type, an opening angle θ =180 degrees gets the maximum value of ΔC_d, while the best opening angle for the Standing Cylinder Type is 210 degrees.

2) The hemisphere shaped cylinder shows the best performance among the Sphere Type.

3) The resistance factor on the roughness fixed on the channel bed depends on both Reynolds number and the relative depth h/k. ΔC_d decrease with the increase of Reynolds number and the relative depth. However, ΔC_d approaches to a constant value when the Reynolds number is above 10^5.

4) From the experimental results for 38 types of
bottom roughness units, it becomes clear that
the most effective shapes are **Type 5** and
Type 6 which are shown in *FIG. 6.*

요   약

폐쇄성 해역에 있어서의 수질개선을 위하여, *Gug et al.*(1997)은 방향성 저항 특성을 가진 저면조도를 이용하여 조석잔차류의 창조와 제어를 통하여 외해와의 해수교환을 활발히 하는 새로운 수질개선법을 제안하였다. 다수의 인공 저면조도를 배치하는 것에 의해서 조석잔차류를 설계하는 것이 가능하다는 것을 알 수 있었다. 이것은 경제적인 관점에서 가능하면 적은 수의 저면조도를 배치하여 최대의 효과를 얻는 것이 필요할 것이다. 본 연구에서는 효과적으로 조석잔차류를 창조하고 제어할 수 있는 기능을

가진 저면조도의 최적 형상을 구하고자 하였다. 먼저, 몇 개의 간단한 형상이 기본형으로서 실험되었으며, 다음으로 이 기본형의 유효한 형상에 기초를 둔 38 종류의 저면조도에 대하여 수리실험을 통하여 그 저항특성을 조사하였다. 결과적으로 수리실험을 행한 수십종의 저면조도의 형상 중에서 2가지 타입이 최적형상으로서 선정되었다.

Reference

1) S., GUG, Komatsu, T., Yano, S., Kohashi, N. (1997) : *Proc. XXXVIIth IAHR Cong.,* San-Francisco, pp. 653-658.
2) Awaya, Y., Komatsu, T.,Kawasaki, S., Asai, K., and Fujita, K. (1995) : *Proc. XXXVIIth IAHR Cong.,* 3, London, pp. 233-238.